

# Estimating the temporal and spatial extent of gene flow among sympatric lizard populations (genus *Sceloporus*) in the southern Mexican highlands

Jared A. Grummer<sup>\*1</sup>, Martha L. Calderón-Espinosa<sup>2</sup>, Adrián Nieto-Montes de Oca<sup>3</sup>, Eric N. Smith<sup>4</sup>, Fausto R. Méndez-de la Cruz<sup>5</sup>, and Adam D. Leaché<sup>1</sup>

<sup>1</sup>Department of Biology and Burke Museum of Natural History and Culture, University of Washington, Box 351800, Seattle, WA 98195-1800, USA

<sup>2</sup>Instituto de Ciencias Naturales, Universidad Nacional de Colombia, Sede Bogotá, Colombia

<sup>3</sup>Museo de Zoología and Departamento de Biología Evolutiva, Facultad de Ciencias, Universidad Nacional Autónoma de México, Ciudad Universitaria, México 04510, Distrito Federal, México

<sup>4</sup>Amphibian & Reptile Diversity Research Center, Department of Biology, University of Texas at Arlington, Arlington, TX 76019-0498

<sup>5</sup>Laboratorio de Herpetología, Instituto de Biología, Universidad Nacional Autónoma de México, Ciudad Universitaria, México, D. F., C. P. 04510, México

August 31, 2014

**Running head:** Temporal and spatial extent of gene flow

---

\*Corresponding author: grummer@uw.edu

## Abstract

Interspecific gene flow is pervasive throughout the tree of life. Although detecting gene flow between populations has been facilitated by new analytical approaches, determining the timing and geography of hybridization has remained difficult, particularly for historical gene flow. A geographically explicit phylogenetic approach is needed to determine the ancestral population overlap. In this study, we performed population genetic analyses, species delimitation, simulations, and a recently developed approach of species tree diffusion to infer the phylogeographic history, timing and geographic extent of gene flow in the *Sceloporus spinosus* group. The two species in this group, *S. spinosus* and *S. horridus*, are distributed in eastern and western portions of Mexico, respectively, but populations of these species are sympatric in the southern Mexican highlands. We generated data consisting of three mitochondrial genes and eight nuclear loci for 148 and 68 individuals, respectively. We delimited six lineages in this group, but found strong evidence of mito-nuclear discordance in sympatric populations of *S. spinosus* and *S. horridus* owing to mitochondrial introgression. We used coalescent simulations to differentiate ancestral gene flow from secondary contact, but found mixed support for these two models. Bayesian phylogeography indicated more than 60% range overlap between ancestral *S. spinosus* and *S. horridus* populations since the time of their divergence. Isolation-migration analyses, however, revealed near-zero levels of gene flow between these ancestral populations. Interpreting results from both simulations and empirical data indicate that despite a long history of sympatry among these two species, gene flow in this group has only recently occurred.

<sup>25</sup> Key words: Mexico, mito-nuclear discordance, Bayesian phylogeography, hybridization,  
<sup>26</sup> gene flow, coalescent simulations, species delimitation

## Introduction

27        The topic of hybridization, or gene flow between evolutionary independent  
28        lineages, has captivated evolutionary biologists for nearly two centuries (Darwin 1859;  
29        Harrison 1993). Gene flow between species is common in nature with approximately  
30        10% and 25% of animal and plant species known to hybridize, respectively (Mallet  
31        2005). Although hybrid zones have been identified across a variety of organisms  
32        (Abbott *et al* 2013; Larson *et al* 2013), determining the temporal and geographic extent  
33        of hybridization has remained a difficult task (Hewitt 2001).

34        Analytical advancements in the field of phylogeography have enabled sophisticated  
35        model-testing approaches, including the ability to test demographic scenarios including  
36        gene flow (Avise 2000; Knowles 2009; Hickerson *et al* 2010). New phylogeographic  
37        methods, and Bayesian phylogeography in particular, infer the geographic diffusion of a  
38        clade over time within a coalescent-based framework and have therefore enabled the  
39        simultaneous estimation of the spatial and temporal history of individuals and  
40        populations (Lemey *et al* 2009, 2010; Nylander *et al* 2014). Whereas the initial  
41        implementation of Bayesian phylogeography required discretized areas (e.g., countries)  
42        and assumed a time-homogeneous process of geographic diffusion (Lemey *et al* 2009),  
43        recent modifications have enabled the analysis of continuous geographic data (e.g.,  
44        latitude/longitude coordinates) and heterogeneous geographic diffusion rates amongst  
45        individuals, and most recently, amongst species (Nylander *et al* 2014). However,  
46        examining species-level phylogeography requires an accurate knowledge of the species  
47        limits. But species limits, particularly within closely related groups of species in the  
48        tropics, are often unknown(e.g., Barley *et al* 2013). Identifying species in an objective  
49        manner is requisite to defining groups for species-level phylogeographic analysis.

50        The timing of sympatry or allopatry amongst ancestral ranges of closely related  
51        lineages can be determined by applying absolute dates to phylogeographic analyses.  
52        Knowing this information is of primary concern when comparing phylogeographic  
53        models of divergence with gene flow vs. a model of secondary contact. For instance, two  
54        species that presently have overlapping distributions might be assumed to be in

55 secondary contact if the ancestral ranges of the species were allopatric (Pettengill &  
56 Moeller 2012). Similarly, determining colonization times in areas of hybridization can  
57 help define times of population expansion when testing models of gene flow (e.g., Smith  
58 *et al* 2011). And finally, understanding the geographic and temporal occurrence of  
59 particular clades along with the geologic history of the study region can help elucidate  
60 the biogeographic mechanisms shaping phylogeographic patterns (e.g., Chiari *et al*  
61 2012).

62 Coalescent simulations are a valuable tool for testing alternative phylogeographic  
63 scenarios (e.g., Knowles 2001; Kuhner 2009; Pelletier & Carstens 2014). Modeling  
64 genetic variation within a coalescent framework enables quantitative tests of alternative  
65 population histories and the estimation of population genetic parameters (e.g., Hudson  
66 2002). The modeled population histories are often generated based on inferences  
67 obtained from geological data (Carstens *et al* 2005), paleoclimatic data (Spellman &  
68 Klicka 2006), or based on previous genetic studies (Tsai & Carstens 2013), and the  
69 parameterizations used in the models can be derived from estimates from empirical data  
70 (Carstens *et al* 2005). The parameter estimates based on the empirical data are then  
71 compared to the distribution of simulated values, allowing for the acceptance or  
72 rejection of each hypothesis. In such a way, a vast majority of phylogeographic models  
73 otherwise indistinguishable when only utilizing empirical data can be reduced to a  
74 reasonable set of candidate models (e.g., Pelletier & Carstens 2014).

75 In this study, we examined temporal and geographic patterns of gene flow to  
76 investigate the phylogeographic history of the *Sceloporus spinosus* group. The *S.*  
77 *spinosus* group consists of two species, *S. spinosus* and *S. horridus* (Wiens & Reeder  
78 1997; Smith & Chiszar 1992) that are broadly distributed throughout xeric habitats in  
79 Mexico (Smith 1939; Cole 1970; Frost 1978). Each species is composed of three  
80 subspecies: *S. s. spinosus*, *S. s. apicalis*, and *S. s. caeruleopunctatus*, and *S. h.*  
81 *horridus*, *S. h. albiventris*, and *S. h. oligoporos* (Frost 1978; Smith & Chiszar 1992).  
82 *Sceloporus spinosus* is primarily found in and near the (eastern) Sierra Madre Oriental  
83 mountain range, whereas *S. horridus* is largely distributed in the lower slopes of the

84 (western) Sierra Madre Occidental mountain range. Similarities in the habitat  
85 preferences of these two species have led to areas of sympatry, and suspected  
86 hybridization, in southern Mexico (Fig. 1).

87 In addition to sharing habitat preferences, *S. spinosus* and *S. horridus* also share  
88 similar morphologies, thus making “attempts at determining phylogenetic relationships  
89 among *spinosus* group species on the basis of classical characteristics of scutellation and  
90 color pattern considerably frustrating” (Cole 1970). In fact, previous researchers have  
91 proposed contact zones in Puebla and Oaxaca to explain the observed morphological  
92 overlap in traits (Frost 1978; Boyer *et al* 1987). Beyond identification of species,  
93 distinguishing between subspecies has also proven to be difficult. For instance, overlap  
94 in quantitative characters exists between *S. spinosus* subspecies (Smith & Chiszar  
95 1992), and intergradation has also been suspected between many of the subspecies (*S. s.*  
96 *spinosus* x *S. s. apicalis*, *S. s. apicalis* x *S. s. caeruleopunctatus*, and *S. h. albiventris* x  
97 *S. h. oligoporos*) (Frost 1978; Smith & Chiszar 1992).

98 We aim to determine the temporal and geographic extent of overlap between *S.*  
99 *spinosus* and *S. horridus* with multi-locus nuclear DNA (nDNA) and mtDNA. We first  
100 used population assignment and species delimitation analyses to identify the number  
101 and geographic boundaries of distinct populations within each species, and then inferred  
102 phylogenetic trees for the nDNA and mtDNA data. We then performed coalescent  
103 simulations to model potential historic phylogeographic scenarios that could have  
104 generated the strong pattern of mito-nuclear discordance that we observed in the  
105 empirical data. In addition to testing models of divergence with gene flow and  
106 secondary (2°) contact, we utilized a new Bayesian phylogeographic approach that  
107 estimates the diffusion of populations through time (Nylander *et al* 2014). This  
108 approach provided us with temporal and spatial information for discriminating between  
109 models of divergence with gene flow vs. 2° contact.

110

## 111 Materials & Methods

112

### Taxon Sampling

113 One hundred forty-eight individuals were sampled across the distributions of *S.*  
114 *horridus* and *S. spinosus* (Fig. 1; Supplemental Table 1). Four samples of *S.*  
115 *edwardtaylori* were included for analysis because recent work (using combined n- and  
116 mtDNA) showed that this taxon is nested within the *S. spinosus* group (Leaché 2010;  
117 Wiens *et al* 2010). Assignment of individuals to species and subspecies was based on  
118 morphological character descriptions by Smith (1939), Smith & Smith (1951), Frost  
119 (1978), and Smith & Chiszar (1992). Of these 152 individuals, 81 yielded nuclear  
120 sequence data. However, after data refinement (see below), a total of 70 individuals,  
121 including two *S. edwardtaylori* individuals, were represented in the nuclear DNA  
122 (nDNA) analyses. Both *S. horridus* and *S. spinosus* were nearly equally represented in  
123 the nDNA dataset (Supplemental Table 2). Three individuals of *Sceloporus clarkii* were  
124 included in our dataset to serve as the outgroup for phylogenetic analyses.

125

### Molecular Data Collection

126 Genomic DNA was extracted from tissue using the Qiagen extraction kit. A total  
127 of three mtDNA regions and eight nDNA loci were targeted for sequencing and analysis;  
128 five of the nDNA regions are protein-coding (BACH1, EXPH5, KIAA\_2018, NKTR, and  
129 R35), one region is intronic (NOS1) and two are anonymous loci. We sequenced  
130 portions of the mitochondrial genes encoding the fourth unit of the NADH  
131 dehydrogenase (ND4, and adjacent genes encoding the tRNAs for histidine, serine, and  
132 leucine; Arèvalo *et al* 1994), the 12S ribosomal gene (Leaché & Reeder 2002), and  
133 cytochrome B (Kocher *et al* 1989).

134 Standard PCR protocols were used to amplify mitochondrial DNA (mtDNA),  
135 whereas a “touch-down” protocol was used to amplify the nDNA regions (94° C for  
136 1:00, [0:30 at 94° C, 0:30 at 61° C, 1:30 at 68° C] x 5 cycles, [0:30 at 94° C, 0:30 at 59°  
137 C, 1:30 at 68° C] x 5 cycles, [0:30 at 94° C, 0:30 at 57° C, 1:30 at 68° C] x 5 cycles, and  
138 [0:30 at 94° C, 0:30 at 50° C, 1:30 at 68° C] for 25 cycles). Diploid nuclear genotypes  
139 were phased using the program PHASE (Stephens *et al* 2001) where alleles were

140 discarded if any site probability was <0.95 (resulting in <20% data reduction). We  
141 tested for intragenic recombination using the difference in sum-of-squares test (McGuire  
142 & Wright 2000) in TOPALi (Milne *et al* 2009) using a step-size of 10bp and a window  
143 size of 100bp for 500 parametric bootstraps.

144

### *Population Assignment*

145 We explored two methods to identify distinct populations within the *S. spinosus*  
146 group that utilize multi-locus nDNA data and require no *a priori* knowledge of  
147 population assignment or number of populations. We used the Bayesian program  
148 STRUCTURAMA (Huelsenbeck & Andolfatto 2007; Huelsenbeck *et al* 2011) to identify  
149 the number of populations (k) present in our data. To ensure that the posterior  
150 distribution was not sensitive to the prior mean value for k, we chose the prior value to  
151 range between 1 and 10, assuming no admixture between populations (assuming  
152 admixture resulted in unstable results, where more populations were inferred than  
153 individuals in our dataset). We ran four replicates of each STRUCTURAMA analysis  
154 for a length of  $10^6$  generations and a burn in of  $2.5 \times 10^5$  (analyses ran for  $2 \times 10^6$ ,  $5 \times 10^6$ ,  
155 and  $10 \times 10^6$  produced similar results; results not shown). We present results as the  
156 arithmetic mean of the four replicate analyses.

157 To estimate the number of populations within a geographic context, we used the  
158 program Geneland (Guillot *et al* 2005a,b; Guillot 2008). This program uses a spatial  
159 statistical model and Markov chain Monte Carlo sampling with GPS coordinates and  
160 multi-locus genotypes to estimate the number of populations, individual assignment  
161 probabilities, and the geographic limits between populations that are in  
162 Hardy-Weinberg equilibrium. We varied the number of populations from 1-10 with a  
163 spatial correlation between allele frequencies, and ran five independent analyses with  
164 the same parameters for  $10^6$  generations. We modified the format of the Geneland  
165 output files and combined the results with the program CLUMPP (Jakobsson &  
166 Rosenberg 2007) to generate individual assignment probabilities.

167

### *Phylogenetic Tree Estimation*

We estimated maximum likelihood phylogenetic trees for each nDNA locus in addition to concatenated nDNA and mtDNA datasets separately to examine the concordance in evolutionary history between these genomes. RAxML (Stamatakis 2006) was used with the GTR +  $\Gamma$  nucleotide substitution model and run for 500 nonparametric bootstrap iterations for both n- and mtDNA analyses, where one out of two alleles was randomly chosen to represent each individual in the concatenated nDNA analysis. Partitioning the data by gene vs. codon position did not affect topology or branch length estimates, so we present results from partitioning by codon position. We ran two replicates of each analysis to ensure stability of our results. Phylogenetic relationships were considered significant when bootstrap (bs) values were > 70% (Hillis & Bull 1993; Alfaro *et al* 2003).

179

### *Bayes Factor Delimitation of Species (BFD)*

To delimit evolutionarily independent lineages, we performed Bayes Factor Delimitation of species (BFD) using only the nDNA dataset (Grummer *et al* 2014). Our species delimitation models were based on a combination of the results from population assignment and migration analyses. Gene flow violates the coalescent model used in the species tree estimation program \*BEAST (Heled & Drummond 2010), so we performed species delimitation on two distinct datasets in an effort to remove potentially admixed individuals located on population margins. One dataset consisted of individuals limited to the “core” range of each population as determined in Geneland (see Results section below), whereas the other dataset consisted of all individuals (Fig. 3). Our expectation was that the dataset consisting of all individuals would be more likely to support the recognition of fewer species because gene flow between populations homogenizes gene pools and makes divergent populations appear as one. Six species delimitation models were tested with each dataset: 1) the six-population model where each population based on population assignment analyses was distinct (the “6 pop” model), 2) a model of five species where the northern and central populations of *S.*

195 *horridus* were lumped together (the “northern *horridus* migration” model), 3) a second  
196 five-species model where central and southern populations of *S. horridus* were lumped  
197 together (the “southern *horridus* migration” model), 4) a third five-species model with  
198 central and southern populations of *S. spinosus* lumped together (the “southern  
199 *spinosus* migration” model), 5) a four-species model with all populations of *S. horridus*  
200 lumped together (the “all *horridus* migration” model), and lastly 6) a two-species  
201 model where the three populations of each *S. horridus* and *S. spinosus* are represented  
202 as a single species (the “2 pop” model). Models 2-5 are based on “lumping” lineages  
203 together that were inferred to have non-zero migration rates between them (see Results  
204 below). We ran \*BEAST with the same settings as in our Bayesian phylogeographic  
205 analyses (below), and selected the best species delimitation model through Bayes factor  
206 (Bf) analysis of the path sampling (“PS”) and stepping stone (“SS”) marginal  
207 likelihood estimates (Baele *et al* 2012). A model is considered significantly better than  
208 the rest if the Bf value is greater than 10 (Kass & Raftery 1995).

#### *Genealogical Sorting Index*

209 We performed simulations to discern whether gene flow occurred amongst  
210 ancestral (i.e., divergence with gene flow) or extant populations (i.e., secondary  
211 contact). To determine when gene flow occurred in the *S. spinosus* group, we used the  
212 genealogical sorting index (gsi). The gsi is a statistic that estimates the degree of  
213 exclusive ancestry of individuals in labeled groups on a rooted tree and is a statistically  
214 more powerful measure of population divergence than  $F_{ST}$  (Cummings *et al* 2008). The  
215 gsi statistic can range from 0 to 1, where the maximum value of 1 is achieved when a  
216 group is monophyletic, and is normalized to account for disparities in group sizes while  
217 also accommodating unresolved relationships (i.e., polytomies). Although genealogical  
218 exclusivity is a function of the sorting of ancestral polymorphisms, allele sharing could  
219 also be due to the extent and timing of migration events. We therefore modeled  
220 migration scenarios and performed coalescent simulations to test models of divergence  
221 with gene flow vs. 2° contact, which have explicit expectations about the timing of  
222 migration events.

223 Coalescent simulations were performed in the program MCcoal (Rannala & Yang  
224 2003; Yang & Rannala 2010). In our simulations, we used a symmetric migration  
225 matrix and held the migration rate constant at 1  $N_e m$  (0.5  $N_e m$  in each direction), but  
226 varied the migration start and end times (Fig. 2). Divergence times and population  
227 sizes used in the simulations were derived from estimates of our empirical data in the  
228 programs BP&P (Yang & Rannala 2010) and Arlequin v3.5 (Excoffier & Lischer 2010),  
229 respectively. We simulated species trees including no gene flow (Scenario A; Fig. 2a),  
230 ancestral gene flow between the common ancestors of *S. horridus* and *S. spinosus*  
231 (Scenario B; Fig. 2b), gene flow between ancestral populations as well as contemporary  
232 gene flow between one *S. horridus* and two *S. spinosus* lineages (lineages selected based  
233 on empirical results, see Results; Fig. 2c), gene flow between the common ancestors of *S.*  
234 *horridus* and *S. spinosus*, followed by a cessation of gene flow until contemporary gene  
235 flow between three lineages as above (Scenario D; Fig. 2d), and contemporary gene flow  
236 between one lineage of *S. horridus* and two lineages of *S. spinosus* (Scenario E; Fig. 2e).  
237 We restricted our simulations of gene flow to these models because the mtDNA clade  
238 showing admixture was comprised only of individuals from these three populations.

239 We simulated 10,000 gene trees under each model, then calculated a gsi value for  
240 each group within each gene tree in the “genealogicalSorting” R package (using the  
241 “multitree” function). We focused empirical gsi calculations on the mtDNA locus in an  
242 attempt to resolve the putative pattern of interspecific gene flow. To account for  
243 phylogenetic uncertainty in the empirical data, we calculated the single (“ensemble”)  
244 gsi value for the mtDNA for each population on a posterior distribution of 8,000 trees  
245 inferred in MrBayes (v3.2; Ronquist and Huelsenbeck 2003). For the MrBayes analysis,  
246 we partitioned the dataset by codon for protein-coding genes (one 12S partition, three  
247 partitions each for CytB, and four partitions for ND4 including the tRNA coding  
248 sequence) and assigned each the best substitution model determined in jModelTest v2  
249 (Darriba *et al* 2012; Guindon & Gascuel 2003). We ran two analyses for  $10^7$   
250 generations, sampling every 2000 steps, and discarded the first 20% as burn-in  
251 (determined by visual examination in Tracer v1.5 Rambaut & Drummond 2007).

252 To assess the probability that the empirical mtDNA gsi values are different from  
253 the gsi values from the simulated trees, we calculated the frequency of simulated gsi  
254 values that were in the tail of the distribution beyond the empirical value. These values  
255 could therefore be interpreted as one-half of the p-value statistic when testing the null  
256 expectation that the empirical mtDNA gsi values were drawn from the simulated gsi  
257 distribution. The comparison of empirical mtDNA gsi values to the simulated gsi values  
258 provide a statistical test of determining the timing of migration events in the *S.*  
259 *spinosus* group.

260

#### *Estimation of Nuclear Gene Flow*

261 We estimated ancestral and contemporary levels of gene flow in the program IMa2  
262 (Hey 2010) using our empirical nDNA. This program estimates bi-directional and  
263 uni-directional migration rates, divergence times, and population sizes. The IM model  
264 assumes non-recombinant loci, constant population sizes, and that population-level  
265 sampling has been performed randomly. We performed analyses on three separate  
266 datasets, where the user-specified topologies were based on our empirical species tree  
267 estimate (see below): (1) only *S. horridus* populations (=3 extant populations), (2)  
268 only *S. spinosus* populations (=3 extant populations), and (3) both *S. horridus* and *S.*  
269 *spinosa* (=6 extant populations). For the three-population models, we specified  $3 \times 10^5$   
270 steps as burn-in with  $3 \times 10^5$  steps following burn-in, and allowed the program to infer  
271 migration rates amongst all pairwise lineage combinations (including ancestral gene  
272 flow). For the 6-population model, the burn-in period lasted for  $5 \times 10^5$  generations  
273 followed by  $3 \times 10^5$  steps post burn-in, and we estimated migration between all pairwise  
274 lineage combinations (including ancestral gene flow). Whereas the three-population  
275 models allowed us to examine gene flow between populations within each species  
276 (including ancestral gene flow), the 6-population model enabled us to test for gene flow  
277 across species (both extant and ancestral lineages). For all models, we ran four  
278 replicate analyses (using different starting seeds) of 100 chains with heating terms of  
279 0.98 and 0.90 (options -ha and -hb). Significant levels of migration were assessed using

280 the Nielsen & Wakeley (2001) test implemented in IMa2.

281

### Bayesian Phylogeographic Analysis

282 We utilized Bayesian phylogeography (Lemey *et al* 2009, 2010) to determine the  
283 temporal and geographic extent of overlap, and therefore the possibility of introgression,  
284 between the populations comprising the “admixed” mtDNA clade. We utilized a  
285 method that was recently developed by Nylander *et al* (2014) that applies the relaxed  
286 random walk (RRW) continuous phylogeographic approach (Lemey *et al* 2010) to relax  
287 the assumption of geographic rate diffusion homogeneity across branches in the species  
288 tree. This method follows a two-tiered approach in the program BEAST (Drummond &  
289 Rambaut 2007) where a posterior distribution of species trees is first generated, which is  
290 then subsequently used in an RRW analysis.

291 To generate the species tree, we used \*BEAST v1.7.5 (Heled & Drummond 2010)  
292 on the 8-locus nuclear dataset, with individuals assigned to lineages based on our  
293 population assignment and BFD results (see Results section below). The species tree  
294 analysis only included individuals that did not show signs of admixture (i.e., we only  
295 included individuals with  $>0.90$  posterior probability for belonging to one population).  
296 We calibrated the root of the (*S. spinosus* group + *S. edwardtaylori*) clade at 5.0 million  
297 years ago (mya) with a standard deviation of 0.5, based on the time-calibrated tree  
298 from Leaché & Sites Jr (2010); this allowed us to place dates on the phylogeographic  
299 events within this group. Each gene was given its own partition and analyzed under the  
300 uncorrelated lognormal molecular clock with the preferred substitution model as  
301 mentioned above. Analyses were run for  $3 \times 10^8$  generations, logging every  $2 \times 10^4$  steps,  
302 and convergence was assessed in Tracer v1.5 (Rambaut & Drummond 2007).

303 The species tree diffusion analysis was performed with BEAST v1.8.1. We used  
304 LogCombiner v1.8 from the BEAST package to combine and thin results from three  
305 independent species tree analyses. After pruning *S. edwardtaylori* in the program  
306 Mesquite (v2.75; Maddison and Maddison 2011), one thousand species trees from the  
307 posterior distribution were then used as input for the species tree diffusion analysis. We

308 circumscribed polygons in Google Earth to approximate extant distributions for each  
309 lineage/population based on published range maps (Smith 1939; Frost 1978; Smith &  
310 Chiszar 1992) and Geneland results; these polygons were then referenced along with the  
311 posterior distribution of species trees for analysis. We explored the effect of  
312 (geographic) starting location on species-level geographic diffusion by choosing two  
313 different starting locations within each species' boundaries. All priors on the RRW  
314 diffusion model were kept the same as in Nylinder et al. (2014). We ran four  
315 independent replicates of species tree diffusion analysis for  $5 \times 10^8$  generations each,  
316 logging every  $5 \times 10^5$  generations. The "time slice" function of the program SPREAD  
317 (Bielejec *et al* 2011) was then used to visualize the ancestral 80% HPD regions in  
318 Google Earth at  $5 \times 10^5$  year intervals from 3.0 - 0.5mya. All files used for Bayesian  
319 phylogeographic analysis are available online as supplementary materials.

320

## Results

### *Taxon Sampling*

321 We generated mtDNA data for 74 *S. horridus*, 74 *S. spinosus*, and four *S.*  
322 *edwardtaylori*. Our nDNA dataset consisted of a subset of the individuals present in the  
323 mtDNA dataset: 36 *S. horridus*, 32 *S. spinosus*, and two *S. edwardtaylori*. All  
324 individuals in the mtDNA dataset were amplified for at least one of the three  
325 mitochondrial regions examined, whereas the final nDNA dataset only consisted of  
326 individuals with sequence data for  $\geq 4$  loci ( $\geq 50\%$  complete matrix).

327

### *Molecular Data Collection*

328 The three mtDNA regions totaled 2,639bp with 859 variable sites, 714 of which  
329 were parsimony-informative (Table 1; GenBank accession nos. xxxx-xxxx). In contrast,  
330 the eight nDNA regions totaled 5,716bp with 459 variable sites and 420  
331 parsimony-informative sites (GenBank accession nos. xxxx-xxxx). Large indels (>10bp)  
332 were present in the intron (NOS1) and two anonymous loci (Sun\_035, Sun\_037), but  
333 these were not scored for usage in the phylogenetic analyses. No evidence of intra-genic

334 recombination was detected in any gene.

335

### *Population Assignment*

336 STRUCTURAMA analyses indicated the highest posterior probability resulted  
337 when partitioning individuals into six populations when the prior on k was  $\leq 6$  (Table  
338 2). When the prior mean on k was  $\geq 7$ , seven populations were inferred in the *S.*  
339 *spinosis* group, indicating some sensitivity of our analysis to the prior distribution on  
340 k. Geneland results provided strong support for six distinct populations where this  
341 model (k=6) received  $>0.65$  of the posterior probability of k values between 1 and 10  
342 across replicate analyses (results not shown). Three of these populations were composed  
343 of *S. horridus* individuals, and the other three populations were composed of *S.*  
344 *spinosis* individuals (Fig. 3). Proportions of population assignment based on Geneland  
345 output are shown in Figure 1. Nearly all individuals (65/68) showed  $>0.95$  probability  
346 in belonging to a single cluster. The geographic boundaries of the populations inferred  
347 in Geneland are largely in agreement with currently recognized subspecific boundaries.

348

### *Phylogenetic Tree Estimation*

349 Phylogenetic trees for six out of the eight nDNA loci revealed moderate to strong  
350 support for the monophyly of one species to the exclusion of the other, whereas the  
351 remaining two loci showed some degree of species-level paraphyly (Supplemental Fig.  
352 1). Support values towards the tips of the trees (i.e., between alleles) were generally  
353 low. The position of *S. edwardtaylori* was variable across gene trees. The concatenated  
354 nDNA tree revealed strong support (bs = 100) for the sister relationship between *S.*  
355 *edwardtaylori* and (*S. spinosus* + *S. horridus*) (Figs. 1,4; Supplemental Fig. 2). The  
356 support for mutual exclusivity between *S. spinosus* and *S. horridus* was strong with bs  
357 values of 99 and 100 for each group, respectively. The nDNA was geographically  
358 structured with strongly supported clades in general agreement with currently  
359 recognized subspecific geographic boundaries (Fig. 4). However, it is important to note  
360 that not all populations inferred in our population assignment tests appear as natural

361 groups in the nDNA concatenated tree, specifically, central *S. horridus* and southern *S.*  
362 *spinosus* (Fig. 4).

363 The (*S. edwardtaylori*, (*S. spinosus*, *S. horridus*)) relationship inferred with the  
364 nDNA is in stark contrast to the relationships inferred with the mtDNA. In the mtDNA  
365 tree, both *S. spinosus* and *S. horridus* were paraphyletic, with *S. edwardtaylori* nested  
366 within these two species with strong support (Figs. 1,4; Supplemental Fig. 3). The  
367 mtDNA tree also shows two clades of *S. spinosus* and two clades of *S. horridus*, in  
368 addition to one moderately supported clade consisting of both *S. spinosus* and *S.*  
369 *horridus* individuals. Interestingly, the *S. spinosus* and *S. horridus* individuals in this  
370 “admixed” clade occur in southern Mexico where these two species are sympatric (Fig.  
371 4). Although these putatively admixed individuals form a clade in the mtDNA tree,  
372 they belong to three distinct populations in the nDNA, specifically, central *S. spinosus*,  
373 southern *S. spinosus*, and southern *S. horridus* (Fig. 4). This phylogeographic result  
374 was interpreted as geographically localized mitochondrial introgression, as incomplete  
375 lineage sorting in the mtDNA would be expected to not leave a strong geographic  
376 signature. We therefore performed coalescent simulations with gene flow and used the  
377 gsi statistic to determine the timing of this admixture.

378

### *Species Delimitation*

379 Marginal likelihood estimates based on both PS and SS marginal likelihood  
380 estimators were very similar, and the ranking of models was identical, so we therefore  
381 only show the PS results. Out of the six species delimitation models examined, the  
382 model containing six species (corresponding to the six populations identified through  
383 population assignment analyses) was favored over all other models by a  $B_f > 70$  (Table  
384 3). This result was consistent across both datasets composed of all samples and “core”  
385 samples. These results did not match our expectation, given that non-zero levels of gene  
386 flow were detected between three population-pairs (see “Estimation of Nuclear Gene  
387 Flow” results below). The “2 pop” model that represented *S. horridus* and *S. spinosus*  
388 each as a single species composed of three populations was the lowest ranked model in

389 both datasets, indicating the strong possibility that currently described subspecies may  
390 warrant the recognition as distinct species.

#### *Genealogical Sorting Index*

391 We focus our gsi results on the central *S. spinosus*, southern *S. spinosus*, and  
392 southern *S. horridus* populations (and their ancestors), because these populations  
393 appeared to be admixed in the mtDNA tree and therefore were the populations in  
394 which we modeled gene flow (see Figs. 2,4). When gene flow was not modeled in our  
395 simulations, gsi values were relatively high (all values  $\geq 0.66$ ; Scenario A; Table 3), i.e.,  
396 relatively high levels of monophyly within populations. The gsi values reported for  
397 Scenario B, which included only historic gene flow between the common ancestors of *S.*  
398 *horridus* and *S. spinosus* (and therefore represents the model of divergence with gene  
399 flow), were similar to (but all less than) those reported for the model with no gene flow  
400 (Scenario A; Table 3; Supplemental Fig. 4), indicating that the gsi index did not do  
401 well at detecting ancestral gene flow. When migration amongst extant populations was  
402 included in the model (e.g., Scenarios C-E), gsi values markedly decreased (Table 3;  
403 Supplemental Fig. 4), particularly for the populations in which migration was modeled,  
404 demonstrating that the gsi statistic does much better at detecting recent gene flow, as  
405 opposed to ancestral gene flow.

406 Based on the empirical mtDNA data, central and southern populations of *S.*  
407 *horridus* along with the central *S. spinosus* population returned the lowest gsi values ( $<$   
408 0.55; Table 3), whereas gsi values for the other populations were all  $\geq 0.90$  (Table 3).  
409 According to our test statistic, the probability that southern *S. horridus* had a history  
410 similar to those modeled by Scenarios A and B is very low (0.0002, and 0.003,  
411 respectively), meaning that this population experienced appreciable levels of ancestral  
412 gene flow ( $> 1N_e m$ ; Fig.2; Table 3). However, there is strong probability that central  
413 and southern *S. spinosus* populations match the history of Scenarios A and B (all  
414  $p \geq 0.09$  for rejecting these scenarios), meaning they experienced negligible levels of  
415 ancestral gene flow ( $< 1N_e m$ ; Table 3). The empirical mtDNA gsi values for southern *S.*  
416 *horridus* and central *S. spinosus* populations strongly matched the simulated

417 distribution values (all  $p > 0.11$  for rejecting these scenarios) when gene flow was  
418 modeled amongst extant lineages (Scenarios C-E; Figs. 2,5; Table 3). However, the  
419 empirical gsi value for the southern *S. spinosus* population did not fit the expected  
420 distribution of simulated gsi values ( $p < 0.03$  for rejecting these scenarios) resulting from  
421 these same scenarios modeling recent gene flow (Fig. 5; Table 3).

422

### *Estimation of Nuclear Gene Flow*

423 Although the 3-population models are nested subsets of the 6-population model,  
424 the IMa2 results were inconsistent between these analyses (Table 4). Significant levels  
425 of unidirectional gene flow were detected within *S. horridus*, from northern *S. horridus*  
426 into southern *S. horridus*, from southern *S. horridus* into central *S. horridus*, and  
427 historically, between the common ancestor of northern and central populations *S.*  
428 *horridus* populations with the southern *S. horridus* population (Table 4). Within *S.*  
429 *spinosus*, significant levels of gene flow were detected from the central *S. spinosus*  
430 population into southern *S. spinosus*, and historically, from northern *S. spinosus* into  
431 the common ancestor of central and southern *S. spinosus* populations (Table 4). The  
432 full 6-population model allowed us to test for gene flow between *S. horridus* and *S.*  
433 *spinosus*. In terms of migration across species, a significant migration rate was reported  
434 from southern *S. horridus* into northern *S. spinosus*, a result coincident with a scenario  
435 of interspecific mitochondrial introgression (Table 4).

436

### *Bayesian Phylogeographic Analysis*

437 Only one (*S. h. horridus*) individual was removed for the species tree analysis due  
438 to an admixed genotype (Fig. 1). The time-calibrated species tree revealed a root age of  
439 3.1 mya (1.55-5.61 95% C.I.) for the *S. spinosus* group (results not shown). Altering the  
440 starting coordinates for each population did not appear to have an affect on our species  
441 tree diffusion analyses. At 3.0 and 2.5 mya, the distributions of the common ancestors  
442 (CA) of *S. horridus* and *S. spinosus* were largely sympatric in southern Mexico (Fig.  
443 6). *Sceloporus horridus* split into two lineages at 2.1 mya, where southern *S. horridus*

444 was nearly 100% sympatric with the *S. spinosus* CA. At 1.5 mya, southern *S. horridus*  
445 had moved slightly to the east and shares less range overlap with the CA of *S. spinosus*.  
446 By 1.0 mya, southern *S. horridus* and the CA of central and southern *S. spinosus*  
447 populations overlap with each other by approximately 60%. At 0.5 mya, the central *S.*  
448 *spinosus* population is nearly 100% sympatric with the southern *S. spinosus* population,  
449 and southern *S. horridus* is sympatric in the east with both central and southern  
450 populations of *S. spinosus* (Fig. 6). These results indicate that all populations present  
451 in the admixed mtDNA clade were largely sympatric throughout their existence until  
452 the past < one million years, at which point populations began diverging in allopatry.

453

## Discussion

454 Recent analytical advancements in gene flow detection have given researchers the  
455 ability to utilize multi-locus datasets to estimate migration not only amongst extant  
456 lineages, but also between ancestral lineages (e.g., Hey 2010). Similarly,  
457 phylogeographic analyses can be tested in a statistical framework (e.g., Chan *et al* 2011;  
458 Pelletier & Carstens 2014). And recently, species trees, as opposed to gene trees, have  
459 become the currency of some phylogeographic approaches (Nylander *et al* 2014).  
460 However, identifying the extent of historic geographic overlap and/or separation of  
461 lineages, parameters critical to differentiating between secondary contact and divergence  
462 with gene flow, has remained difficult (e.g., Pettengill & Moeller 2012). In this study,  
463 we employed phylogeographic and coalescent-based simulation approaches to determine  
464 two parameters that are often difficult to infer, particularly for ancestral lineages: the  
465 timing and geographic extent of gene flow.

466

### *Phylogeography of the S. spinosus Group*

467 A number of phylogeographic studies have been performed in Mexico due to its  
468 rich orogenic history (e.g., Devitt 2006; Bryson *et al* 2011a; Bryson Jr *et al* 2012a;  
469 Leaché *et al* 2013), and many studies have found that the major mountain ranges  
470 (Sierra Madre Occidental, western Mexico; Sierra Madre Oriental, eastern Mexico;

471 Trans-Mexican Volcanic Belt, southern-central Mexico; Sierra Madre del Sur, southern  
472 Mexico) have had major effects on the biogeographic patterns across many taxonomic  
473 groups (e.g., Bryson Jr *et al* 2012b; Ruiz-Sanchez & Specht 2013). On the other hand,  
474 some researchers argue that some of these features do not represent single biogeographic  
475 entities (e.g., Corona *et al* 2007). Although the extant distribution of *S. spinosus* group  
476 taxa is similar to other species (e.g., *Phrynosoma orbiculare*; Bryson Jr *et al* 2012),  
477 subtleties in habitat (and therefore elevational) preferences result in a unique  
478 phylogeographic distribution across Mexico for this group, particularly in the geographic  
479 overlap of distinct populations in southeastern Mexico (but see Fernández 2011).

480 Population assignment and species delimitation analyses identified six independent  
481 lineages within the *S. spinosus* group (Fig. 3; Table 2); geographic distributions largely  
482 coincide with the ranges of subspecies (Figs. 1,3). The geographic boundaries of these  
483 lineages appear to be strongly influenced by the geology of the region. In southwestern  
484 Mexico, the Rio Santiago, Rio Ahuijullo, and the western portion of the Balsas basins  
485 form the interface between *S. horridus* populations 1 and 2 (Fig. 3). These barriers  
486 have also been implicated in lineage divergence of horned lizards (*Phrynosoma*;  
487 Bryson Jr *et al* 2012b) and rattlesnakes (*Crotalus*; Bryson *et al* 2011a). Similarly, the  
488 Trans-Mexican Volcanic Belt corresponds to the north-south barrier separating  
489 northern and central *S. spinosus* populations. That this geologic feature is a natural  
490 barrier causing population differentiation is no surprise, as many peaks in this range are  
491 >5000m and habitats are widely varied (Marshall & Liebherr 2000). The low elevation  
492 valleys between the Trans-Mexican Volcanic Belt and Sierra Madre del Sur in  
493 northwestern Oaxaca and eastern Puebla likewise seem to be isolating southern  
494 populations of *S. spinosus*, a pattern seen in other lizard species (Bryson & Riddle  
495 2012).

496 The time-calibrated species tree indicated that the common ancestor of *S.*  
497 *spinosus* and *S. horridus* diverged approximately 3.1 mya (Fig. 6). This is in agreement  
498 with Cole's (1970) hypothesis that these two species originated in the late Pliocene.  
499 Since this time, Mexico has gone through a number of glacial and pluvial (precipitation)

500 cycles causing range expansions and contractions and population coalescence and  
501 divergence of many species (Hewitt 2004). Ancestral *S. spinosus* and *S. horridus*  
502 populations were isolated to the Central Mexican Plateau and western slope of the  
503 Sierra Madre Occidental, respectively, likely due to Pleistocene glacial cycles (Riddle &  
504 Hafner 2006). Following separation, pluvial climates allowed the northern and central  
505 populations of *S. horridus* to be “in more-or-less continuous contact with each other”  
506 (Frost 1978).

507 The prolonged extent of geographic overlap between ancestral lineages of *S.*  
508 *horridus* and *S. spinosus* provided ample opportunity for genetic exchange between  
509 these lineages. However, our simulation results showed that little to no ancestral gene  
510 flow occurred in this region (for two out of three lineages modeled; Table 3), which  
511 refutes the model of divergence with gene flow. The lack of ancestral gene flow, in spite  
512 of our phylogeographic results, could be for a few reasons. First, the ancestral locations  
513 of these lineages was incorrectly reconstructed. The method of species tree geographic  
514 diffusion is new (Nylander *et al* 2014) and has not been tested under simulation, and we  
515 are therefore unaware of any inaccuracies it may have. Furthermore, the ancestral  
516 locations the method is allowed to explore are limited to the geographic extent of extant  
517 distributions (or however else the researcher chooses to draw the population-delimiting  
518 polygons prior to analysis). Simulations and further empirical studies must be  
519 performed with this method to determine its accuracy. Secondly, individuals within the  
520 reconstructed ancestral ranges may have been occupying the (small) regions  
521 allopatric/parapatric to the other species. This is possible, however, not likely, as the  
522 regions in allopatry are peripheral and small in comparison with each lineages’ entire  
523 range. Third, although ancestral *S. spinosus* and *S. horridus* may have been broadly  
524 sympatric, they may have not been syntopic. Both species currently inhabit mostly  
525 xeric habitats, but show different microhabitat preferences (Cole 1970), meaning they  
526 simply may have not historically come into contact. And lastly, perhaps species-specific  
527 recognition cues were more pronounced due to reinforcement as ancestral populations  
528 diverged. Frost (1978) noted a northwest-southeast cline in *S. h. albiventris/S. h.*

529 *oligoporus* populations for some external morphological characters (e.g., color  
530 patterning) that he posited was due to reinforcement at the subspecific boundary. Such  
531 a situation could be a strong barrier to ancestral gene flow.

532 The phylogeographic model of 2° contact is the most likely given our results, in  
533 concert. The simulation modeling 2° contact (Scenario E; Fig. 2) fit the empirical data  
534 for southern populations of both *S. spinosus* and *S. horridus*, although the empirical  
535 data for southern *S. spinosus* (population 3) did not fit the results from this scenario.  
536 Only one “*S. spinosus* south” individual was recovered in the admixed mtDNA clade,  
537 potentially indicating a low level of gene flow that did not match the simulations  
538 modeling a higher migration rate for this taxon. The split of the common ancestor of  
539 southern *S. spinosus* populations into its daughter lineages did not occur until around  
540 860,000 years ago. After this point, the ranges of southern *S. horridus* and *S. spinosus*  
541 shared a moderate amount of range overlap in southern Mexico where much of the  
542 admixed mtDNA clade is situated (Figs. 4,6). The patterns of, or lack thereof, nDNA  
543 ancestral gene flow detected in the IMa2 analyses further support the 2° contact model.  
544 No ancestral gene flow was detected between *S. spinosus* and *S. horridus* common  
545 ancestors, but was detected between extant populations of *S. spinosus* and *S. horridus*  
546 (Table 4). Although a new study by Leaché *et al* (2013a) found evidence for divergence  
547 with gene flow between *S. horridus* and *S. spinosus*, the method they used did not allow  
548 for discernment between models of secondary contact vs. divergence with gene flow.

549

#### *Mito-nuclear Discordance in the S. spinosus Group*

550 Numerous studies have reported conflicting evolutionary histories between nuclear  
551 and mitochondrial genomes (“mito-nuclear discordance”, reviewed in Toews & Brelsford  
552 2012). Out of 126 studies identified by Toews & Brelsford (2012) that documented  
553 strong incongruence between mt- and nDNA biogeographic patterns, the overwhelming  
554 majority of cases (97%) reported that the discordance likely arose from geographic  
555 isolation followed by secondary contact; the most common form of mito-nuclear  
556 discordance is due to the asymmetric movement of mtDNA between lineages. In the

557 case of the *S. spinosus* group, we can safely rule out the possibility that incomplete  
558 lineage sorting (ILS) of mtDNA alleles as the cause of mito-nuclear incongruence, as we  
559 would expect ILS to leave a geographically-independent genealogical signature. We  
560 cannot, however, rule out the possibility that adaptive introgression may be a factor,  
561 particularly because many of the individuals belonging to the "admixed" mtDNA clade  
562 were collected in moderately high elevation sites (>2000m) where individuals with  
563 particular mitochondrial haplotypes may be better adapted (e.g., Cheviron & Brumfield  
564 2009).

565 The most likely cause of mito-nuclear discordance in the *S. spinosus* group  
566 appears to be due to unidirectional gene flow from southern *S. spinosus* and *S. horridus*  
567 into central *S. spinosus*. The admixed mtDNA clade is composed of central *S. spinosus*,  
568 southern *S. spinosus*, and southern *S. horridus* individuals (Figs. 1,4). Whereas  
569 southern *S. horridus* and *S. spinosus* individuals were recovered in other mitochondrial  
570 clades, all central *S. spinosus* individuals were confined to the admixed clade. This  
571 phylogenetic pattern intimates that the admixed mtDNA clade was originally composed  
572 of all central *S. spinosus* individuals, and recently, that southern *S. horridus* and *S.*  
573 *spinosus* males have introgressed their mtDNA copies into central *S. spinosus* females.  
574 Our gsi results support the notion of recent (mitochondrial) gene flow between southern  
575 *S. horridus* and central *S. spinosus*, but not between southern *S. spinosus* and central  
576 *S. spinosus* (Table 3).

577

### *Population Distinctiveness and Divergence Within the Sceloporus spinosus Group*

578 Previous authors have claimed that no clear boundaries exist between species, or  
579 even subspecies, within the *S. spinosus* group. For instance, Boyer *et al* (1987)  
580 concluded that *S. s. spinosus* and *S. h. horridus* were conspecific based on the overlap  
581 of femoral pores and contact frequency of supraocular-median head scales as a result of  
582 intergradation. Smith & Chiszar (1992) later returned *S. spinosus* and *S. horridus* to  
583 specific status after a reinterpretation of these individuals as intergrades between *S. s.*  
584 *spinosus* and *S. s. apicalis*. Distinguishing between *S. spinosus* subspecies is also

585 problematic due to the slight difference in average values of quantitative characters  
586 between subspecies, where Smith & Chiszar (1992) note that examination only of a  
587 series of six or more permits "reasonably secure identifications". Similar problems exist  
588 within *S. horridus*, where Frost (1978) reported a large area of intergrade in western  
589 Mexico between *S. h. albiventris* and *S. h. oligoporos*. Notwithstanding, Lemos-Espinal  
590 *et al* (2004) regarded these taxa as distinct species. In summary, distinguishing between  
591 what have been considered as distinct taxa in the *S. spinosus* group, is problematic,  
592 and little agreement exists between previous authors.

593 Contrary to some previous research (Wiens & Reeder 1997; Smith 2001), the  
594 results of our nDNA-based phylogeny show the *S. spinosus* group to be monophyletic  
595 (to the exclusion of *S. edwardtaylori*; Fig. 4). Furthermore, *S. spinosus* and *S. horridus*  
596 are monophyletic with respect to each other, a result at odds with previous research  
597 (Wiens *et al* 2010). This discrepancy is certainly due to the overriding signal of the  
598 mtDNA in the combined mt- and nDNA analysis of Wiens *et al* (2010). Lineages are  
599 often determined to be distinct based on an assessment of gene flow levels, a test of the  
600 biological species concept (Mayr 1942; Mayr *et al* 1963). Our tests of nuclear gene flow  
601 in the *S. spinosus* group revealed gene flow not only between populations of each  
602 species, but also across species (Table 4). But, the level of gene flow we detected in all  
603 instances was far below  $0.5 N_e m$ , a value used by some when determining species limits  
604 (Porter 1990; Hey 2009). The interpretation of these results, particularly for the  
605 6-population model, should be cautioned because the size of our molecular dataset is  
606 likely inadequate to generate accurate results (Hey 2010; Choi & Hey 2011).

607 We based our species delimitation models on a combination of results from  
608 population assignment and migration analyses. In an attempt to account for gene flow,  
609 which has been shown to severely affect parameter estimation in coalescent-based species  
610 tree analyses (Leaché 2009; Leaché *et al* 2013b), we excluded individuals located near  
611 population boundaries (Fig. 3). This of course assumes that the gene flow we detected  
612 occurred on population boundaries, an assumption which may not be true. Removing  
613 these peripheral individuals did not affect our species delimitation results that indicated

614 the presence of six independent lineages in the *S. spinosus* group. Even though the  
615 simulations results from Grummer *et al* (2014) showed the BFD method to be effective  
616 at selecting the true species history when compared to falsely “lumping” lineages, we  
617 interpret these results with caution. A few instances have been reported with this  
618 method that select the model with the largest number of lineages (e.g., Bryson Jr *et al*  
619 2014), indicating a potentially systematic problem with this method to delimit species.  
620 However, this needs to be explored with further simulations.

621 When comparing gsi values between our coalescent simulations and empirical  
622 mtDNA, it appears that the empirical data for the southern *S. horridus* population are  
623 most in agreement with scenarios modeling recent, but not ancestral, gene flow across  
624 species (Scenarios C-E; Fig. 2; Table 3). On the other hand, the empirical data of the  
625 southernmost *S. spinosus* population are in agreement with a scenario in which there  
626 was either no gene flow, or ancestral gene flow between *S. spinosus* and *S. horridus*  
627 ancestors. The gsi simulation results did not reject any scenario for the central *S.*  
628 *spinosus* population (Table 3). Our conclusions based on the gsi results are directly a  
629 function of the levels of gene flow used in our simulations. We used a relatively high  
630 migration value of  $1 N_e m$  in our simulations ( $0.5 N_e m$  unidirectionally from each  
631 population, where  $N_e m$  = the product of the effective population size and the migration  
632 rate per generation), where some researchers consider a migration rate of  $N_e m > 0.5$   
633 enough to keep populations from diverging (Porter 1990). We therefore believe that we  
634 have modeled a realistic level of gene flow to assess matrilineal-based migration in the  
635 *S. spinosus* group.

636

### *Conclusions*

637 The number of plausible models that should be evaluated in phylogeographic  
638 studies is nearly infinite (e.g., Tsai & Carstens 2013; Pelletier & Carstens 2014). Here,  
639 we generated a small number of plausible models based on the results from our  
640 empirical data. Given our results, we conclude that i) six independent genetic lineages  
641 exist in the *S. spinosus* group, and identifying species is important for accurately

642 modeling evolutionary histories, ii) coalescent simulations reject a model of ancestral  
643 gene flow in the *S. spinosus* group, iii) the Bayesian phylogeographic reconstruction for  
644 the ancestral ranges of the *S. spinosus* group suggests that species within the group  
645 broadly overlapped throughout a majority of their evolutionary history (~3 million  
646 years), and iv) mitochondrial introgression is localized spatially, and likely temporally  
647 as well. The contrasting evolutionary histories of the nuclear and mitochondrial  
648 genomes seem to indicate another example of the mtDNA locus not accurately  
649 representing the true species-level evolutionary history. However, the mitochondrial  
650 genome has nonetheless provided a valuable piece of information in determining the  
651 evolutionary history of the *S. spinosus* group by presenting evidence for the timing and  
652 geographic extent of contact between distinct populations in this group.

### *Acknowledgments*

This work was facilitated through the use of advanced computational, storage, and networking infrastructure provided by the Hyak supercomputer system at the University of Washington through grant support from the National Science Foundation (DEB-1144630) to ADL. MC was supported by a DGEP PhD and DGAPA postdoctoral scholarships from the Universidad Nacional Autónoma de México (UNAM). Financial support was provided by a grant from the UNAM to FMC (PAPIIT IN2009-01) and the American Museum of Natural History through the Theodore Roosevelt Memorial Grants program. Further support for this project was provided by grants from DGAPA, UNAM (PAPIIT no. IN224009) and CONACYT (no. 154093) to A. Nieto-Montes de Oca. We thank the Museo de Zoología Alfonso L. Herrera (MZFC) and the Colección Nacional de Anfibios y Reptiles (CNAR), UNAM, for the loan of specimens and to MZFC for providing tissue samples. Norma Manríquez and Laura Márquez provided useful advice on lab work. J. C. Barajas, E. Pérez Ramos, R. Meza, G. Zamora, A. Ortega, S. López, V. Serrano, N. Martínez, C. Peña and G. Barrios assisted with field work.

## References

- Abbott R, Albach D, Ansell S, *et al* (2013) Hybridization and speciation. *Journal of Evolutionary Biology*, **26**, 229–246.
- Alfaro ME, Zoller S, Lutzoni F (2003) Bayes or bootstrap? a simulation study comparing the performance of bayesian markov chain monte carlo sampling and bootstrapping in assessing phylogenetic confidence. *Molecular Biology and Evolution*, **20**, 255–266.
- Arèvalo E, Davis SK, Sites JW (1994) Mitochondrial dna sequence divergence and phylogenetic relationships among eight chromosome races of the *Sceloporus grammicus* complex (phrynosomatidae) in central mexico. *Systematic Biology*, **43**, 387–418.
- Avise JC (2000) *Phylogeography: the history and formation of species*. Harvard University Press.
- Baele G, Lemey P, Bedford T, Rambaut A, Suchard MA, Alekseyenko AV (2012) Improving the accuracy of demographic and molecular clock model comparison while accommodating phylogenetic uncertainty. *Molecular biology and evolution*, **29**, 2157–2167.
- Barley AJ, White J, Diesmos AC, Brown RM (2013) The challenge of species delimitation at the extremes: diversification without morphological change in philippine sun skinks. *Evolution*, **67**, 3556–3572.
- Bielejec F, Rambaut A, Suchard MA, Lemey P (2011) Spread: Spatial phylogenetic reconstruction of evolutionary dynamics. *Bioinformatics*.
- Boyer T, Smith H, Casas-Andreu G (1987) The taxonomic relationships of the mexican lizard species *Sceloporus horridus*. *Bulletin of the Maryland Herpetological Society*, **18**, 189–191.

Bryson RW, García-Vázquez UO, Riddle BR (2011a) Phylogeography of middle american gophersnakes: mixed responses to biogeographical barriers across the mexican transition zone. *Journal of Biogeography*, **38**, 1570–1584.

Bryson RW, Murphy RW, Lathrop A, Lazcano-Villareal D (2011b) Evolutionary drivers of phylogeographical diversity in the highlands of mexico: a case study of the *Crotalus triseriatus* species group of montane rattlesnakes. *Journal of Biogeography*, **38**, 697–710.

Bryson RW, Riddle BR (2012) Tracing the origins of widespread highland species: a case of neogene diversification across the mexican sierras in an endemic lizard. *Biological Journal of the Linnean Society*, **105**, 382–394.

Bryson Jr RW, García-Vázquez UO, Riddle BR (2012a) Diversification in the mexican horned lizard *Phrynosoma orbiculare* across a dynamic landscape. *Molecular phylogenetics and evolution*, **62**, 87–96.

Bryson Jr RW, García-Vázquez UO, Riddle BR (2012b) Relative roles of neogene vicariance and quaternary climate change on the historical diversification of bunchgrass lizards (*Sceloporus scalaris* group) in mexico. *Molecular phylogenetics and evolution*, **62**, 447–457.

Bryson Jr RW, Linkem CW, Dorcas ME, *et al* (2014) Multilocus species delimitation in the *crotalus triseriatus* species group (serpentes: Viperidae: Crotalinae), with the description of two new species. *Zootaxa*, **3826**, 475–496.

Carstens B, Degenhardt J, Stevenson A, Sullivan J (2005) Accounting for coalescent stochasticity in testing phylogeographical hypotheses: modelling pleistocene population structure in the idaho giant salamander *dicamptodon aterrimus*. *Molecular Ecology*, **14**, 255–265.

Chan LM, Brown JL, Yoder AD (2011) Integrating statistical genetic and geospatial methods brings new power to phylogeography. *Molecular phylogenetics and evolution*, **59**, 523–537.

- Cheviron ZA, Brumfield RT (2009) Migration-selection balance and local adaptation of mitochondrial haplotypes in rufous-collared sparrows (*Zonotrichia capensis*) along an elevational gradient. *Evolution*, **63**, 1593–1605.
- Chiari Y, van der Meijden A, Mucedda M, Lourenço JM, Hochkirch A, Veith M (2012) Phylogeography of sardinian cave salamanders (genus *Hydromantes*) is mainly determined by geomorphology. *PloS one*, **7**, e32332.
- Choi SC, Hey J (2011) Joint inference of population assignment and demographic history. *Genetics*, **189**, 561–577.
- Cole CJ (1970) Karyotypes and evolution of the *spinosis* group of lizards in the genus *Sceloporus*. *American Museum Novitates*, **2431**, 1–47.
- Corona AM, Toledo VH, Morrone JJ (2007) Does the trans-mexican volcanic belt represent a natural biogeographical unit? an analysis of the distributional patterns of coleoptera. *Journal of Biogeography*, **34**, 1008–1015.
- Cummings MP, Neel MC, Shaw KL (2008) A genealogical approach to quantifying lineage divergence. *Evolution*, **62**, 2411–2422.
- Darriba D, Taboada GL, Doallo R, Posada D (2012) jmodeltest 2: more models, new heuristics and parallel computing. *Nature Methods*, **9**, 772–772.
- Darwin C (1859) *The origin of species by means of natural selection: or, the preservation of favored races in the struggle for life*. John Murray.
- Devitt TJ (2006) Phylogeography of the western lyresnake (*Trimorphodon biscutatus*): testing aridland biogeographical hypotheses across the Nearctic–Neotropical transition. *Molecular Ecology*, **15**, 4387–4407.
- Drummond AJ, Rambaut A (2007) Beast: Bayesian evolutionary analysis by sampling trees. *BMC evolutionary biology*, **7**, 214.

Excoffier L, Lischer HE (2010) Arlequin suite ver 3.5: a new series of programs to perform population genetics analyses under linux and windows. *Molecular ecology resources*, **10**, 564–567.

Fernández JA (2011) *Comparative biogeography of the arid lands of Central Mexico*. Ph.D. thesis, Louisiana State University.

Frost D (1978) *Geographic variation and evolution of Sceloporus horridus Wiegmann (Lacertilia: Iguanidae)*. Master's thesis, Louisiana State University.

Grummer JA, Bryson Jr RW, Reeder TW (2014) Species delimitation using bayes factors: simulations and application to the *Sceloporus scalaris* species group (squamata: Phrynosomatidae). *Systematic Biology*, **63**, 119–133.

Guillot G (2008) Inference of structure in subdivided populations at low levels of genetic differentiation—the correlated allele frequencies model revisited. *Bioinformatics*, **24**, 2222–2228.

Guillot G, Estoup A, Mortier F, Cosson JF (2005a) A spatial statistical model for landscape genetics. *Genetics*, **170**, 1261–1280.

Guillot G, Mortier F, Estoup A (2005b) Geneland: a computer package for landscape genetics. *Molecular Ecology Notes*, **5**, 712–715.

Guindon S, Gascuel O (2003) A simple, fast, and accurate algorithm to estimate large phylogenies by maximum likelihood. *Systematic biology*, **52**, 696–704.

Harrison RG (1993) *Hybrid zones and the evolutionary process*. Oxford University Press.

Heled J, Drummond AJ (2010) Bayesian inference of species trees from multilocus data. *Molecular biology and evolution*, **27**, 570–580.

Hewitt G (2004) Genetic consequences of climatic oscillations in the quaternary. *Philosophical Transactions of the Royal Society of London. Series B: Biological Sciences*, **359**, 183–195.

Hewitt GM (2001) Speciation, hybrid zones and phylogeography—or seeing genes in space and time. *Molecular Ecology*, **10**, 537–549.

Hey J (2009) On the arbitrary identification of real species. *Speciation and Patterns of Diversity* (eds Butlin RK, Bridle J, Schlüter D), pp. 15–28.

Hey J (2010) Isolation with migration models for more than two populations. *Molecular biology and evolution*, **27**, 905–920.

Hickerson M, Carstens B, Cavender-Bares J, et al (2010) Phylogeography's past, present, and future: 10 years after. *Molecular Phylogenetics and Evolution*, **54**, 291–301.

Hillis DM, Bull JJ (1993) An empirical test of bootstrapping as a method for assessing confidence in phylogenetic analysis. *Systematic biology*, **42**, 182–192.

Hudson RR (2002) Generating samples under a wright–fisher neutral model of genetic variation. *Bioinformatics*, **18**, 337–338.

Huelsenbeck JP, Andolfatto P (2007) Inference of population structure under a dirichlet process model. *Genetics*, **175**, 1787–1802.

Huelsenbeck JP, Andolfatto P, Huelsenbeck ET (2011) Structurama: Bayesian inference of population structure. *Evolutionary bioinformatics online*, **7**, 55.

Jakobsson M, Rosenberg NA (2007) Clumpp: a cluster matching and permutation program for dealing with label switching and multimodality in analysis of population structure. *Bioinformatics*, **23**, 1801–1806.

Kass RE, Raftery AE (1995) Bayes factors. *Journal of the american statistical association*, **90**, 773–795.

Knowles LL (2001) Did the pleistocene glaciations promote divergence? tests of explicit refugial models in montane grasshoppers. *Molecular Ecology*, **10**, 691–701.

Knowles LL (2009) Statistical phylogeography. *Annual Review of Ecology, Evolution, and Systematics*, **40**, 593–612.

Kocher TD, Thomas WK, Meyer A, et al (1989) Dynamics of mitochondrial dna evolution in animals: amplification and sequencing with conserved primers. *Proceedings of the National Academy of Sciences*, **86**, 6196–6200.

Kuhner MK (2009) Coalescent genealogy samplers: windows into population history. *Trends in Ecology & Evolution*, **24**, 86–93.

Larson EL, White TA, Ross CL, Harrison RG (2013) Gene flow and the maintenance of species boundaries. *Molecular Ecology*.

Leaché A, Sites Jr J (2010) Chromosome evolution and diversification in north american spiny lizards (genus *sceloporus*). *Cytogenetic and genome research*, **127**, 166–181.

Leaché AD (2009) Species tree discordance traces to phylogeographic clade boundaries in north american fence lizards (*sceloporus*). *Systematic Biology*, p. sys057.

Leaché AD (2010) Species trees for spiny lizards (genus *Sceloporus*): Identifying points of concordance and conflict between nuclear and mitochondrial data. *Molecular phylogenetics and evolution*, **54**, 162–171.

Leaché AD, Harris RB, Maliska ME, Linkem CW (2013a) Comparative species divergence across eight triplets of spiny lizards (*sceloporus*) using genomic sequence data. *Genome biology and evolution*, **5**, 2410–2419.

Leaché AD, Harris RB, Rannala B, Yang Z (2013b) The influence of gene flow on species tree estimation: a simulation study. *Systematic biology*, p. syt049.

Leaché AD, Palacios JA, Minin VN, Bryson RW (2013) Phylogeography of the trans-volcanic bunchgrass lizard (*Sceloporus bicanthalis*) across the highlands of south-eastern mexico. *Biological Journal of the Linnean Society*, **110**, 852–865.

- Leaché AD, Reeder TW (2002) Molecular systematics of the eastern fence lizard (*Sceloporus undulatus*): a comparison of parsimony, likelihood, and bayesian approaches. *Systematic biology*, **51**, 44–68.
- Lemey P, Rambaut A, Drummond AJ, Suchard MA (2009) Bayesian phylogeography finds its roots. *PLoS computational biology*, **5**, e1000520.
- Lemey P, Rambaut A, Welch JJ, Suchard MA (2010) Phylogeography takes a relaxed random walk in continuous space and time. *Molecular biology and evolution*, **27**, 1877–1885.
- Lemos-Espinal J, Chiszar D, Smith H, Woolrich-Piña G (2004) Selected records of 2003: lizards from chihuahua and sonora, mexico. *Bulletin of the Chicago Herpetological Society*, **39**, 164–168.
- Maddison W, Maddison D (2011) Mesquite 2.75: a modular system for evolutionary analysis.
- Mallet J (2005) Hybridization as an invasion of the genome. *Trends in Ecology & Evolution*, **20**, 229–237.
- Marshall C, Liebherr J (2000) Cladistic biogeography of the mexican transition zone. *Journal of biogeography*, **27**, 203–216.
- Mayr E (1942) *Systematics and the origin of species, from the viewpoint of a zoologist*. Harvard University Press.
- Mayr E, et al (1963) Animal species and evolution. *Animal species and their evolution*.
- McGuire G, Wright F (2000) Topal 2.0: improved detection of mosaic sequences within multiple alignments. *Bioinformatics*, **16**, 130–134.
- Milne I, Lindner D, Bayer M, et al (2009) Topali v2: a rich graphical interface for evolutionary analyses of multiple alignments on hpc clusters and multi-core desktops. *Bioinformatics*, **25**, 126–127.

- Nielsen R, Wakeley J (2001) Distinguishing migration from isolation: a markov chain monte carlo approach. *Genetics*, **158**, 885–896.
- Nylinder S, Lemey P, De Bruyn M, et al (2014) On the biogeography of centipeda: A species-tree diffusion approach. *Systematic biology*, **63**, 178–191.
- Pelletier TA, Carstens BC (2014) Model choice for phylogeographic inference using a large set of models. *Molecular ecology*.
- Pettengill JB, Moeller DA (2012) Phylogeography of speciation: allopatric divergence and secondary contact between outcrossing and selfing *Clarkia*. *Molecular Ecology*, **21**, 4578–4592.
- Porter AH (1990) Testing nominal species boundaries using gene flow statistics: the taxonomy of two hybridizing admiral butterflies (limenitis: Nymphalidae). *Systematic Biology*, **39**, 131–147.
- Rambaut A, Drummond A (2007) Tracer v1. 4.
- Rannala B, Yang Z (2003) Bayes estimation of species divergence times and ancestral population sizes using dna sequences from multiple loci. *Genetics*, **164**, 1645–1656.
- Riddle B, Hafner D (2006) A step-wise approach to integrating phylogeographic and phylogenetic biogeographic perspectives on the history of a core north american warm deserts biota. *Journal of Arid Environments*, **66**, 435–461.
- Ronquist F, Huelsenbeck JP (2003) Mrbayes 3: Bayesian phylogenetic inference under mixed models. *Bioinformatics*, **19**, 1572–1574.
- Ruiz-Sanchez E, Specht CD (2013) Influence of the geological history of the trans-mexican volcanic belt on the diversification of nolina parviflora (asparagaceae: Nolinoideae). *Journal of Biogeography*, **40**, 1336–1347.
- Smith CI, Tank S, Godsoe W, et al (2011) Comparative phylogeography of a coevolved community: concerted population expansions in joshua trees and four *Yucca* moths. *PloS one*, **6**, e25628.

Smith E (2001) *Species boundaries and evolutionary patterns of speciation among the malachite lizards formosus group of the genus Sceloporus (Squamata: Phrynosomatidae)*. Ph.D. thesis, University of Texas at Arlington.

Smith H (1939) *The Mexican and Central American Lizards of the Genus Sceloporus*, vol. 26 of *Zoological Series*. Field Museum Press.

Smith H, Chiszar D (1992) *Sceloporus horridus* and *S. spinosus* (reptilia: Sauria) are separate species. *Bulletin of the Maryland Herpetological Society*, **2**, 44–52.

Smith P, Smith H (1951) A new lizard (*Sceloporus*) from oaxaca, mexico. *Proceedings of the Biological Society of Washington*, **64**, 101–104.

Spellman GM, Klicka J (2006) Testing hypotheses of pleistocene population history using coalescent simulations: phylogeography of the pygmy nuthatch (*Sitta pygmaea*). *Proceedings of the Royal Society B: Biological Sciences*, **273**, 3057–3063.

Stamatakis A (2006) Raxml-vi-hpc: maximum likelihood-based phylogenetic analyses with thousands of taxa and mixed models. *Bioinformatics*, **22**, 2688–2690.

Stephens M, Smith NJ, Donnelly P (2001) A new statistical method for haplotype reconstruction from population data. *The American Journal of Human Genetics*, **68**, 978–989.

Toews DP, Brelsford A (2012) The biogeography of mitochondrial and nuclear discordance in animals. *Molecular Ecology*, **21**, 3907–3930.

Tsai YHE, Carstens BC (2013) Assessing model fit in phylogeographical investigations: an example from the north american sandbar willow salix melanopsis. *Journal of Biogeography*, **40**, 131–141.

Wiens JJ, Kuczynski CA, Arif S, Reeder TW (2010) Phylogenetic relationships of phrynosomatid lizards based on nuclear and mitochondrial data, and a revised phylogeny for *Sceloporus*. *Molecular Phylogenetics and Evolution*, **54**, 150–161.

Wiens JJ, Reeder TW (1997) Phylogeny of the spiny lizards (*Sceloporus*) based on molecular and morphological evidence. *Herpetological Monographs*, pp. 1–101.

Yang Z, Rannala B (2010) Bayesian species delimitation using multilocus sequence data. *Proceedings of the National Academy of Sciences*, **107**, 9264–9269.

Data Accessibility:

- DNA Sequences: Genbank accession nos. xxxx-xxxx
- Bayesian phylogeography species tree .xml provided at Dryad doi:
- All collecting locality information is available in the Supplementary Materials section.

Author Contributions

All authors designed the research and collected specimens; JAG and MLC obtained the data and conducted analyses; JAG wrote the paper, and all co-authors contributed to editing the manuscript.

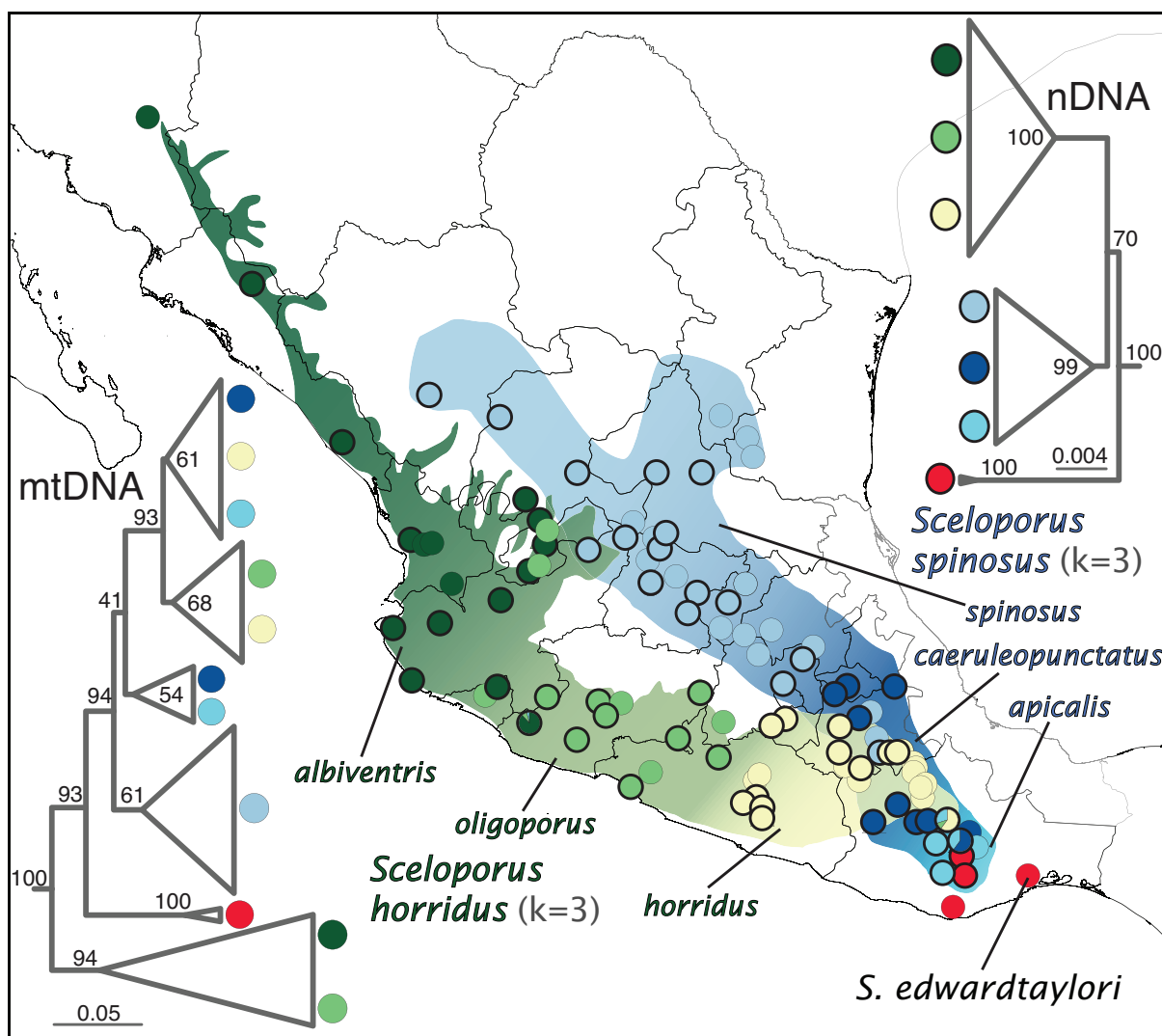


Figure 1: Sampling localities and species/subspecies distributions of *Sceloporus spinosus* and *S. horridus* in Mexico (based on (Smith 1939; Frost 1978; Smith & Chiszar 1992)). Sampling localities with bold rings indicate specimens that have been amplified for nDNA in addition to mtDNA, whereas samples with a light ring have only mtDNA. The designation (i.e., color) of nDNA samples was based on Geneland assignments (3 inferred populations for each species), and the designation of mtDNA samples to subspecies was based on morphological characters. Also shown are the concatenated mt- and nDNA trees inferred from RAxML, where values at nodes represent bootstrap proportions. Note the mixed clade of *S. horridus* and *S. spinosus* in the mtDNA tree, in addition to the contrasting phylogenetic placement of *S. edwardtaylori* between mt- and nDNA trees.

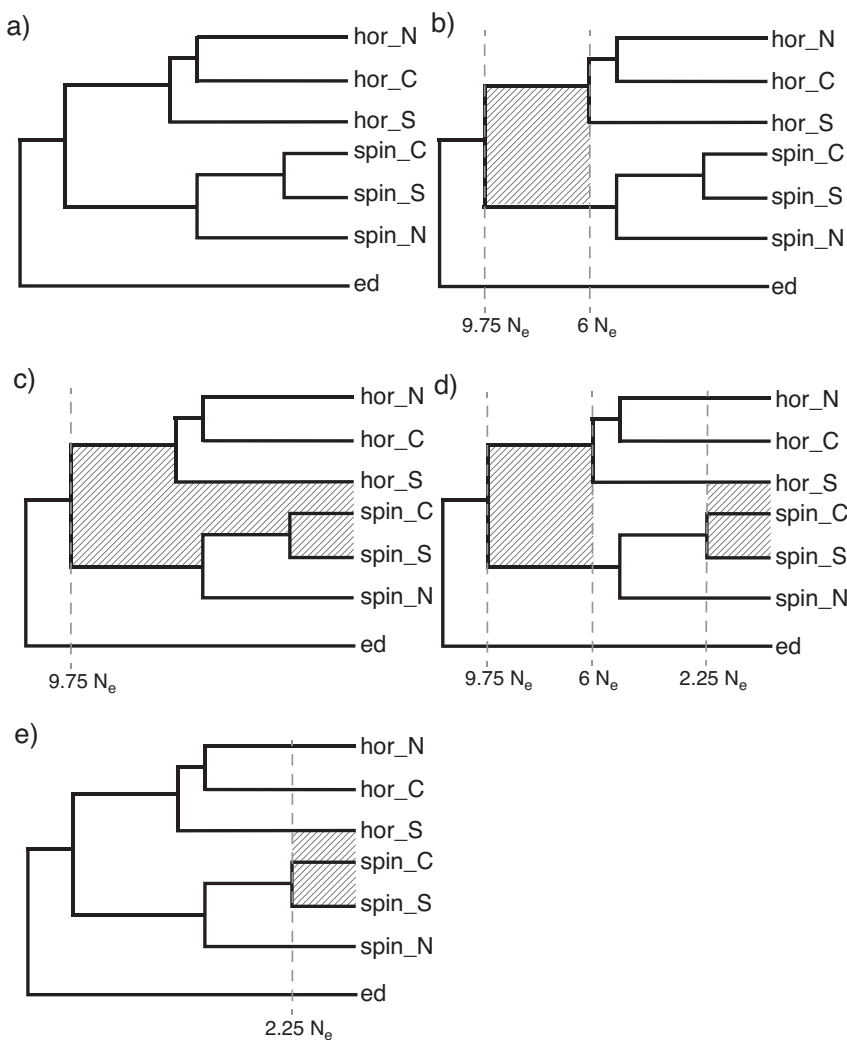


Figure 2: The six scenarios modeled for coalescent-based simulations. Migration times are indicated in coalescent units, and migration events are indicated by diagonal shading. Northern, central, and southern populations are denoted by “N”, “C”, and “S”, respectively.

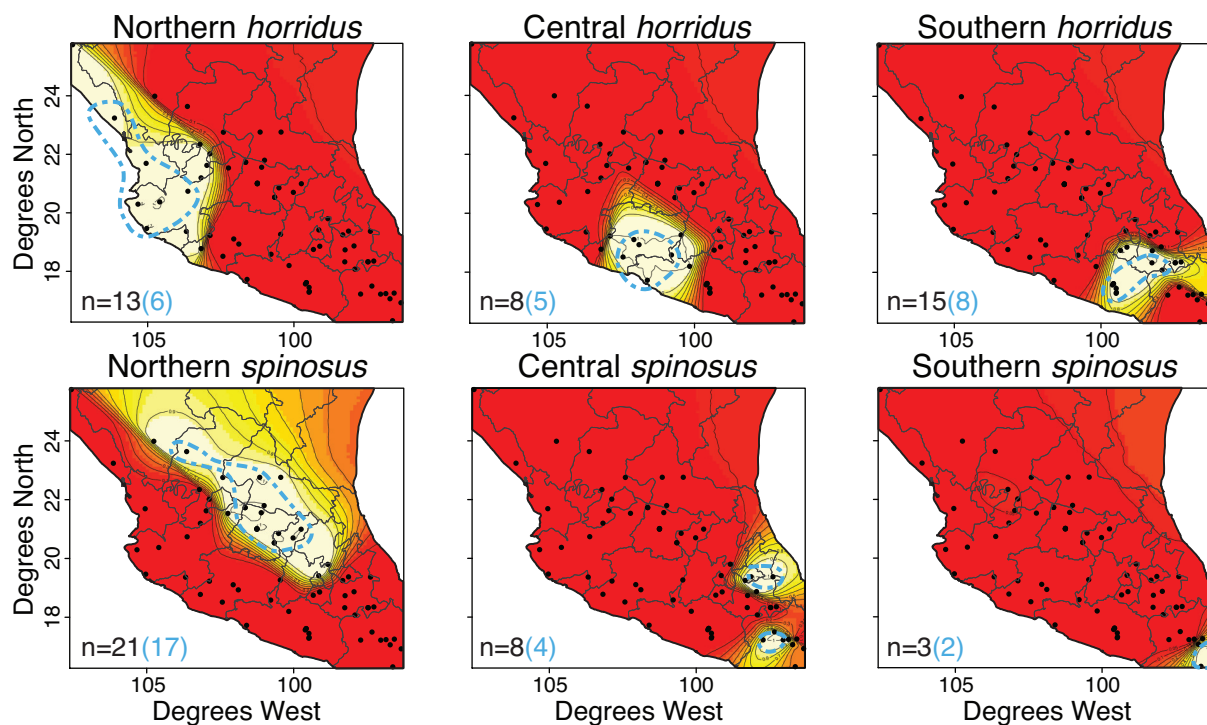


Figure 3: Geneland analysis results showing the number of populations and the probability of individual assignment to each population. These results can be interpreted as topographic maps, where white colors indicate high probabilities of assignment to that cluster and red represents low assignment probability. Blue dashed lines indicate which samples were included in the “core” sampling for BFD analyses. Black numbers in the lower left portion of each tile are the number of individuals in that cluster, whereas the blue number represents the number of individuals from that cluster in the “core” sampling scheme.

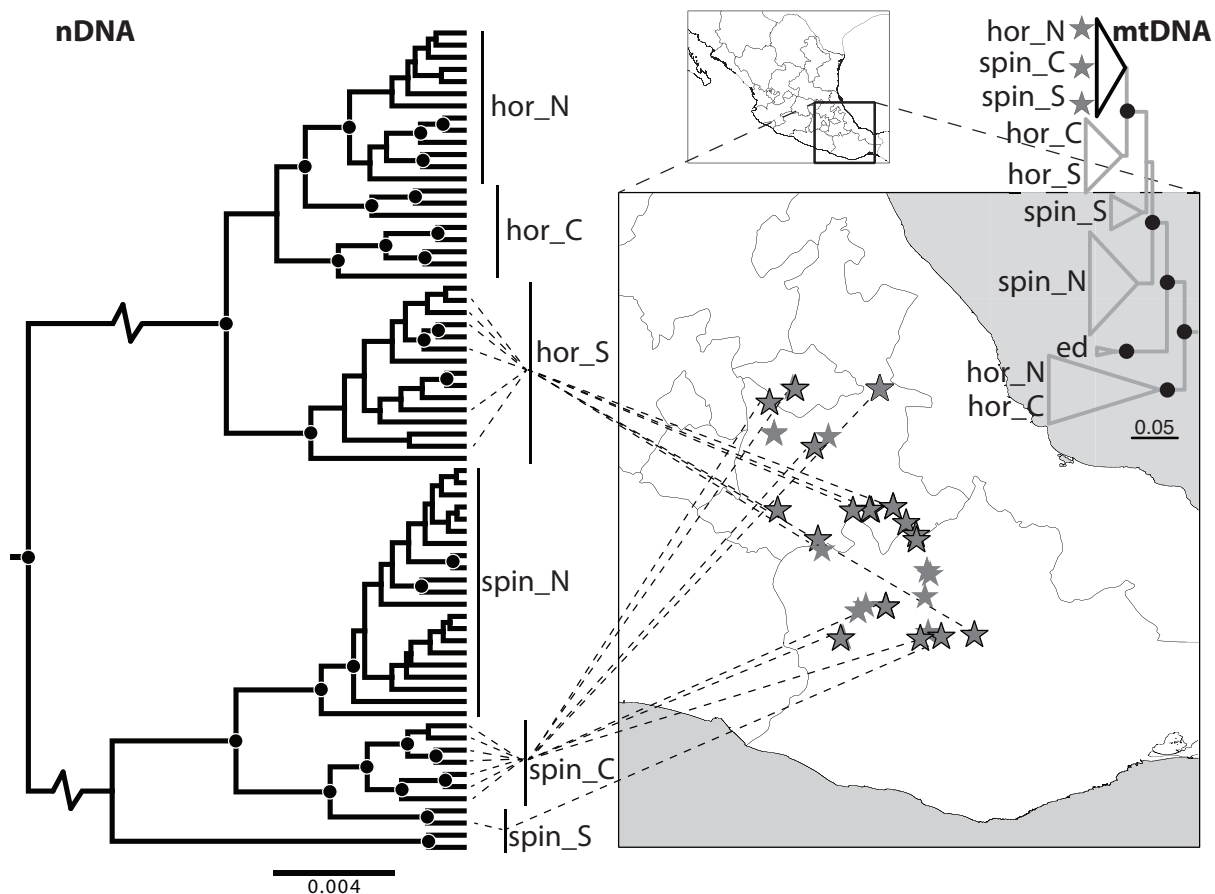


Figure 4: Map showing geographic locations of putatively admixed individuals in south-eastern Mexico along with their phylogenetic positions in n- and mtDNA trees. Stars without bold outlines indicate individuals without nDNA data, and black dots in the phylogenetic trees indicate bootstrap values >70. Note that groupings identified on the nDNA tree are based on population assignment analyses and therefore are not all monophyletic groups (e.g., central *S. horridus* and southern *S. spinosus*).

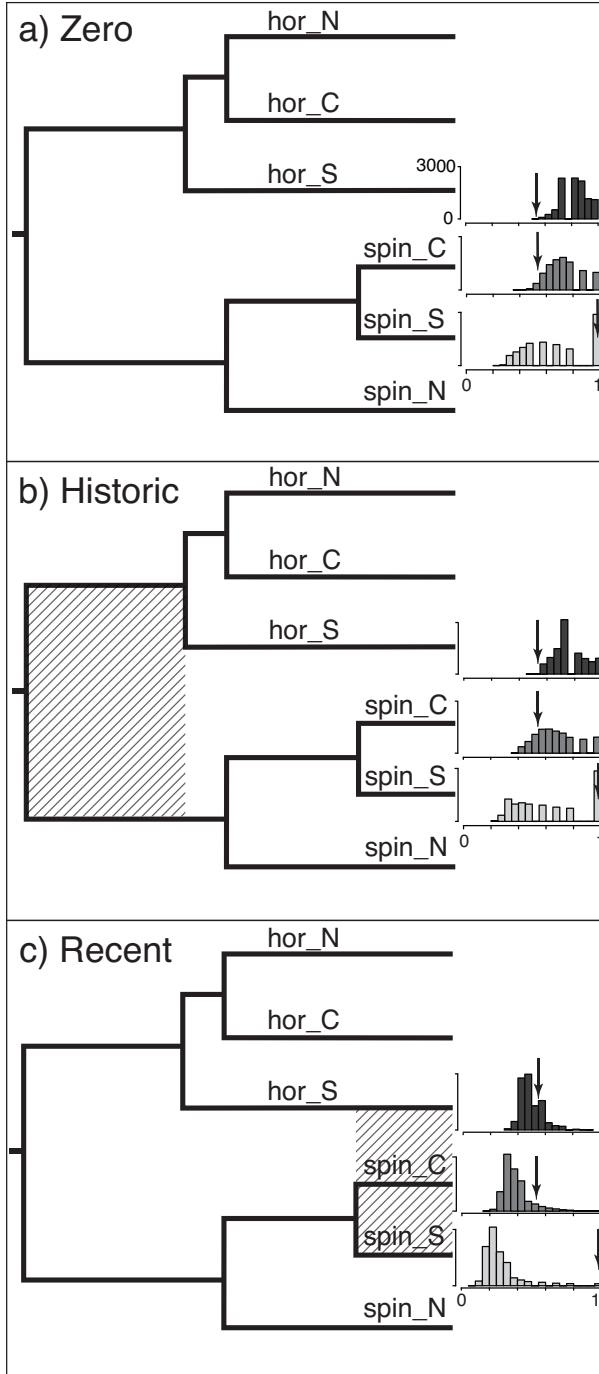


Figure 5: Gsi (genealogical sorting index) results for both simulated and empirical datasets along with the species tree topology used in the simulations. Histograms to the right indicate the distribution of gsi values recorded during simulations (see text for simulation details) for central *Sceloporus spinosus*, southern *S. spinosus*, and southern *S. horridus*. Y-axis values range from 0-3000, and x-axis values of the gsi statistic range from 0-1. Red arrows indicate the gsi value for the mtDNA empirical data. Figure (a) shows the gsi results for the model with no migration (Scenario A), (b) represents historic gene flow only (Scenario B), and (c) represents the gsi values for Scenario E that models recent gene flow (histograms for Scenarios C,D looked nearly identical).

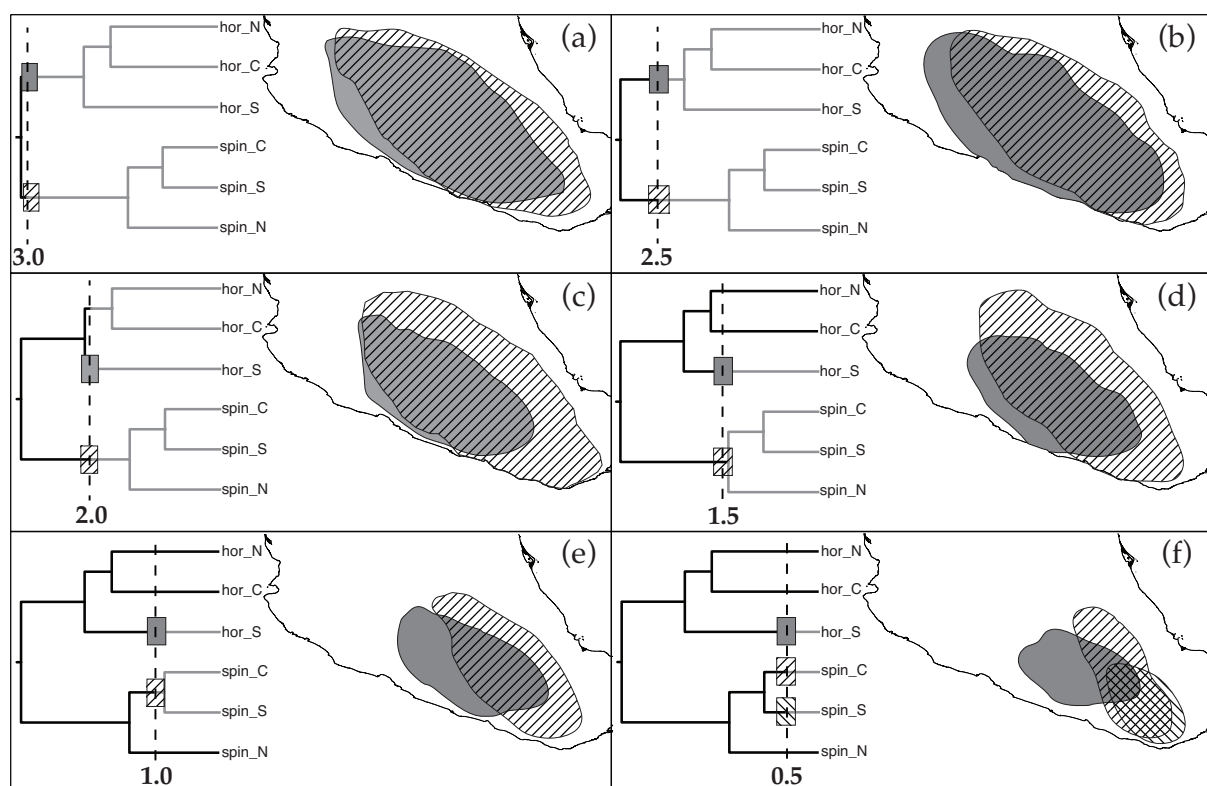


Figure 6: Bayesian phylogeographic results under the relaxed random walk (RW) species tree diffusion approach. Distributions indicate the 80% HPD location of the depicted lineages from 3.0 (a) to 0.5 mya (f) using the “time slice” feature in SPREAD.

Table 1: Information for the genetic data gathered in this study. The first three regions are mitochondrial regions, whereas the remainder are nuclear regions. Gene region “Type” abbreviations indicate noncoding (NC), protein-coding (PC), intron (I), and anonymous (A).

Gene Region	Type	Length (bp)	Variable Sites	Parsimony-Informative Sites	DNA Substitution Model
12S	NC	782	141	113	HKY+I+Γ
CytB	PC	1025	412	352	HKY+I
ND4	PC	832	306	249	HKY+I+Γ
BACH1	PC	1247	91	83	HKY+I
EXPH5	PC	900	55	49	HKY+Γ
KIAA	PC	621	27	25	HKY+I
NKTR	PC	617	54	48	HKY+I
NOS1	I	666	68	66	HKY+Γ
R35	PC	658	43	35	HKY+I
Sun_035	A	522	49	46	HKY+I
Sun_037	A	485	72	68	HKY+Γ
Total	—	8,355	1,318	1,134	—

Table 2: Results from STRUCTURAMA indicating the posterior probability values when the prior mean on the number of populations (k) was varied. Values shown are the average of four independent runs. Bold values indicate the highest posterior probability for each prior mean on k.

Number of Populations	Prior Mean on Number of Populations (k)									
	1 <sup>1</sup>	2	3	4	5	6	7	8	9	10
1	0.00	0.00	0.00	0.00	0.00	0.00	0.00	0.00	0.00	0.00
2	0.00	0.00	0.00	0.00	0.00	0.00	0.00	0.00	0.00	0.00
3	0.00	0.00	0.00	0.00	0.00	0.00	0.00	0.00	0.00	0.00
4	0.00	0.01	0.00	0.00	0.00	0.00	0.00	0.00	0.00	0.00
5	0.00	0.21	0.10	0.05	0.04	0.02	0.01	0.01	0.01	0.01
6	0.00	<b>0.68</b>	<b>0.67</b>	<b>0.60</b>	<b>0.52</b>	<b>0.45</b>	0.38	0.31	0.27	0.22
7	0.00	0.10	0.21	0.30	0.37	0.41	<b>0.45</b>	<b>0.46</b>	<b>0.46</b>	<b>0.45</b>
8	0.00	0.00	0.02	0.05	0.07	0.11	0.15	0.19	0.22	0.26
9	0.00	0.00	0.00	0.00	0.01	0.01	0.02	0.03	0.05	0.06
10	0.00	0.00	0.00	0.00	0.00	0.00	0.00	0.01	0.01	0.01

<sup>1</sup> Results from the analysis with a k prior of 1 were unstable and reported a posterior probability of 1.0 for 68 populations

Table 3: Results from Bayes Factor Delimitation of species (BFD) analyses. Path sampling (“PS”) and stepping stone marginal likelihood estimates were very similar, so we only show the PS results here. See Materials and Methods section for the composition of each species delimitation model.

Model	# Species	All Samples		“Core” Samples	
		PS	Bayes Factor	PS	Bayes Factor
6 pop	6	-12854	—	-11353	—
southern <i>spinosa</i> migration	5	-12889	71	-11396	86
northern <i>horridus</i> migration	5	-12971	234	-11425	144
southern <i>horridus</i> migration	5	-12978	248	-11428	151
all <i>horridus</i> migration	4	-13181	654	-11536	367
2 pop	2	-13419	1129	-11714	721

Table 4: Gsi values for both empirical (mtDNA) and simulated datasets for all scenarios modeled (see Fig. 2). Northern, central, and southern populations are denoted by “N”, “C”, and “S”, respectively. Numbers in parentheses indicate the frequency of simulation results more extreme than the empirical gsi value.

Lineage	mtDNA	Simulations				
		Scenario A	Scenario B	Scenario C	Scenario D	Scenario E
N <i>horridus</i>	0.90	0.81	0.76	0.76	0.77	0.81
C <i>horridus</i>	0.37	0.78	0.74	0.74	0.74	0.78
S <i>horridus</i>	0.54	0.82 (0.0002)	0.76 (0.003)	0.50 (0.248)	0.50 (0.262)	0.50 (0.245)
N <i>spiniferus</i>	1.00	0.93	0.91	0.90	0.91	0.93
C <i>spiniferus</i>	0.53	0.73 (0.045)	0.67 (0.216)	0.39 (0.059)	0.39 (0.063)	0.39 (0.072)
S <i>spiniferus</i>	0.97	0.66 (0.289)	0.63 (0.286)	0.27 (0.010)	0.27 (0.011)	0.27 (0.011)

Table 5: Significant results from the isolation-migration (IMa2) analyses. Values given are in  $2Nm$ , and N/A indicate that no significant migration estimates were reported for that model (e.g., 3-population or 6-population model). Northern, central, and southern populations are denoted by “N”, “C”, and “S”, respectively. Common ancestors of two lineages are indicated with an underscore (\_) between daughter lineage population numbers (e.g., *horridus* N\_C is the common ancestor of northern and central *S. horridus* populations). Asterisks indicate significance levels for the Nielsen & Wakeley (2001) test.

Lineage	3-population Models	6-population Model
Extant		
<i>horridus</i> N —> <i>horridus</i> S	0.132*** <sup>1</sup>	0.67***
<i>horridus</i> S —> <i>horridus</i> C	0.124*	N/A
<i>spinosus</i> C —> <i>spinosus</i> S	0.197*	N/A
<i>horridus</i> S —> <i>spinosus</i> N	N/A	0.024*
Ancestral		
<i>horridus</i> N_C —> <i>horridus</i> S	3.537*	N/A
<i>spinosus</i> N —> <i>spinosus</i> C_S	0.365*	N/A

<sup>1</sup> \*p<0.05; \*\*\*p<0.001